Published in final edited form as:
J Am Chem Soc. 2007 January 10; 129(1): 77–83. doi:10.1021/ja064902x.

Brilliant Sm, Eu, Tb, and Dy Chiral Lanthanide Complexes with Strong Circularly Polarized Luminescence

Stéphane Petoud[†,‖], **Gilles Muller**[‡], **Evan G. Moore**[†], **Jide Xu**[†], **Jurek Sokolnicki**[§], **James P. Riehl**[§], **Uyen N. Le**[‡], **Seth M. Cohen**[†,⊥], and **Kenneth N. Raymond**[†]

†*Contribution from the Department of Chemistry, University of California, Berkeley, California 94720*

‡*Department of Chemistry, San José State University, One Washington Square, San José, California, 95192*

§*Department of Chemistry, University of Minnesota, Duluth, Minnesota 55812*

Abstract

The synthesis, characterization, and luminescent behavior of trivalent Sm, Eu, Dy, and Tb complexes of two enantiomeric, octadentate, chiral, 2-hydroxyisophthalamide ligands are reported. These complexes are highly luminescent in solution. Functionalization of the achiral parent ligand with a chiral 1-phenylethylamine substituent on the open face of the complex in close proximity to the metal center yields complexes with strong circularly polarized luminescence (CPL) activity. This appears to be the first example of a system utilizing the same ligand architecture to sensitize four different lanthanide cations and display CPL activity. The luminescence dissymmetry factor, g_{lum}, recorded for the Eu(III) complex is one of the highest values reported, and this is the first time the CPL effect has been demonstrated for a Sm(III) complex with a chiral ligand. The combination of high luminescence intensity with CPL activity should enable new bioanalytical applications of macromolecules in chiral environments.

Introduction

The structures of proteins, nucleic acids, and other organic molecules are essential information for an understanding of their function in vivo and hence critical for biochemistry, biology, and molecular biology. The ability to identify different protein conformations is one example of this need, since protein folding is strongly determinant in subsequent function. Recent pertinent examples include the role of a malfolded cellular prion protein in transmissible spongiform encephalopathies[1] (e.g., BSE or “mad cow disease”) and the influence of different protein conformations on subsequent spider silk properties.[2]

Circularly polarized luminescence (CPL) is one of the most sensitive techniques that can be used to determine a protein’s conformation in solution, using a luminescent probe that reports on its chiral environment.[3,4,23] Ideally, this technique should combine both the general sensitivity of fluorescence with the advantage of high specificity for CPL signals. Due to their long emission lifetimes and sharp emission bands, luminescent complexes, primarily based on Tb(III) and Eu(III), have proven to be very good luminescence probes for CPL applications. As examples, the conformational changes in calcium and iron binding proteins have been investigated using Tb(III) and Eu(III) ions as structural probes, a proof of principle that

E-mail: raymond@socrates.berkeley.edu.
‖Current address: Department of Chemistry, Chevron Science Center, 219 Parkman Ave., Pittsburgh, PA 15260.
⊥Current address: Department of Chemistry and Biochemistry, University of California, San Diego, 9500 Gilman Dr., La Jolla, CA 92093.

measurements such as these provide highly specific local information on the chiral environment of the lanthanide metal ion.[5,6] This information is thus a crucial complement to that obtained through the analogous but much less sensitive chirooptical absorption technique, circular dichroism (CD), which is often used to determine macromolecular information such as a protein's secondary and tertiary structure.[7,8]

Due to the lanthanides' electronic structure, their complexes have unique optical properties, including luminescence lifetimes that range from micro- to milliseconds, and sharp emission bands whose width at half-height (fwhm) rarely exceed 10 nm.[9-11] This is much narrower than the typically broad fluorescence arising from organic molecule or Cd/Se nanoparticles.[12] As a result of these unique properties, well-designed lanthanide complexes can be used as luminescent probes to analyze biological problems, where a targeted analyte may be present in a matrix that can also contain a large number of other fluorescent molecules (i.e., high background autofluorescence). Similarly, discrimination of the relevant fluorescent signal from that present in biological media (e.g., fluorescence from amino acids such as tyrosine or tryptophan) is readily achieved by time gating (a time-resolved measurement).[13] Indeed, the combination of temporal and spectral discrimination properties have led to the development of time-resolved fluoroimmunoassays with very high sensitivities,[14] without the need for tedious prior purification of the sample which is useful when a very large number of samples must be screened.

Because the lanthanide *f-f* transitions are Laporte forbidden,[13] the molar absorptivity is very low. The typical strategy to circumvent this is to increase the luminescence excitation by coordinating the luminescent lanthanide ion to a chromophore, which acts as an antenna to effectively transfer light energy to the metal.[15,16] For example, in biological systems, amino acids such as tryptophan have been utilized for this purpose, although in that case the binding environment is not optimized for the lanthanide cation.[6,17] In order to form luminescent lanthanide complexes with CPL activity, chiral complexes have been developed where the coordination geometry around the lanthanide is well-defined and controllable, which enables finetuning of the photophysical properties.[18]

Despite these attractive features, there is a limited number of lanthanide based luminescent probes suitable for practical CPL applications in solution. The reason is the weak CPL signal intensity for the complexes described in the literature, due to a combination of limitations imposed by key requirements which must be fulfilled in order to obtain efficient luminescent complexes with detectable CPL signals in solution. First, the limited absorption of lanthanide cations must be overcome by coordinating a ligand that is able to harvest significant amounts of UV or visible light and then efficiently transfer this electronic energy to the lanthanide metal ion. Second, since the excited states of the lanthanide cations can be easily deactivated through nonradiative interaction with their chemical environment (coupling to vibrational modes of solvent molecules or of the ligand), the lanthanide must be protected from this quenching environment when bound to the ligand. This implies that the ligand must fulfill the high coordination number requirement of the lanthanide cation by providing an adequate number of donor atoms (typically between 8 and 12 in solution). Third, the ensuing complex must have sufficient thermodynamic stability and/or kinetic inertness at the appropriate concentration to interact with, and report on, the macromolecule of interest, since dissociation would lead to loss of the antenna effect and a subsequent decrease in luminescence. Fourth, to observe an unambiguous CPL signal it is preferable that only a single enantiomer of the chiral complex be present in solution or, more specifically, the existence of only one of these enantiomers must match the time scale of the experiment (microseconds to milliseconds depending on the nature of the lanthanide cation). Hence, any type of exchange between the complex and the environment in the luminescence time scale should be avoided. Ideally, a rigid, nonfluxional complex, with a saturated coordination sphere, should best satisfy this latter condition.

We have reported the properties of a new family of lanthanide complexes formed with ligands incorporating 2-hydroxyisophthalamide as the chelating unit.[19] Upon coordination, these complexes demonstrate several superior luminescence properties, including highly efficient transfer of electronic excitation from the ligand to metal center and sufficient protection of the lanthanide metal ion against nonradiative deactivation from the environment (e.g., solvent molecules). Indeed, the quantum yield of the Tb(III) complex in H_2O, 61%, is the highest value yet reported for a luminescent metal complex with high stability in aqueous solution. In addition, these newly developed ligands allow the sensitization of four different trivalent lanthanides emitting in the visible (Sm, Eu, Tb, and Dy) with the same ligand. Herein, we have extended the superior luminescence properties of these complexes to CPL activity by the addition of a chiral substituent to the open face of an octadentate, tetrapodal ligand framework, utilizing the 2-hydroxyisophthalamide chelating unit as the sensitizer. This strategy results in the formation of enantiomerically pure complexes with strong circular dichroism (CD) activity. Significantly, these complexes are also strongly luminescent, emitting in the visible region, and display strong CPL activity. As a result of their brightness and improved signal-to-noise ratio, these complexes present new possibilities for increased sensitivity of assays based on CPL measurements. While the Tb(III) complex reported here is the most fluorescent, the strongest CPL effect has been observed for the Eu(III) complex, with one of the highest ΔI values reported to date. In addition, the Dy(III) and Sm(III) complexes are also luminescent and have significant CPL activity, a unique feature which enables us to have four different luminescent probes that can be easily discriminated from each other. Since the sharp emission bands do not appreciably overlap, multiplex detection is possible.

Experimental Section

Synthesis

N,*N*,*N*’,*N*’-Tetrakis(2-aminoethyl)ethane-1,2-diamine (H22) was prepared according to a literature procedure.[20] Unless stated otherwise, all other reagents were purchased from commercial suppliers and used as supplied.

2-Methoxy-bis(2-mercaptothiazolide)isophthalic Acid

2-Methoxyisophthalic acid (20 mmol), 2-mercaptothiazoline (40 mmol), and a catalytic amount of 4-dimethylaminopyridine (20 mg) were dissolved in 150 mL of CH_2Cl_2 under a nitrogen atmosphere. To this was added 1,3-dicyclohexylcarbodiimide (40 mmol), and the solution gradually became yellow in color. After stirring for 5 h, the reaction mixture was filtered, and the filtrate evaporated to dryness to afford a yellow oil. Recrystallization from hot ethyl acetate gave a bright yellow microcrystalline solid. Yield: 55%. IR (film from $CDCl_3$) ν 1229, 1684, 2955 cm^{-1}. ^1H NMR (300 MHz, $CDCl_3$, 25 °C): δ 3.42 (t, J = 7.3 Hz, 4H, CH_2), 3.89 (s, 3H, CH_3), 4.60 (t, J = 7.3 Hz, 4H, CH_2), 7.13 (t, J = 7.7 Hz, 1H, Ar*H*), 7.43 (d, J = 7.6 Hz, 2H, Ar*H*). ^{13}C NMR (400 MHz, $CDCl_3$, 25 °C): δ 29.2, 55.6, 62.9, 123.1, 128.1, 131.9, 154.7, 167.1, 200.8. Anal. Calcd (Found) for $C_{15}H_{14}N_2O_3S_4 \cdot 0.25H_2O$: C, 44.70 (44.75); H, 3.63 (3.53); N, 6.95 (6.82) %.

Me_4(H22IAM)(2-mercaptothiazolide)$_4$

N,*N*,*N*’,*N*’-Tetrakis(2-aminoethyl)ethane-1,2-diamine (H22) (2.8 mmol) dissolved in 150 mL of CH_2Cl_2 was added dropwise to a solution of excess 2-methoxy-bis(2-mercaptothiazolide) isophthalic acid in 600 mL of CH_2Cl_2. The reaction mixture was stirred for ca. 24 h and then evaporated to dryness yielding a yellow oil which was purified by flash chromatography on silica gel (0-15% MeOH in CH_2Cl_2 gradient). The solvent was evaporated to give the product as a yellow foam. Yield: 83.8%. IR (film from CH_2-Cl_2) ν 1522, 1653, 2942 cm^{-1}. ^1H NMR (500 MHz, $CDCl_3$, 25 °C): δ 2.67 (s, 4H, CH_2), 2.71 (t, J = 6.2 Hz, 8H, CH_2), 2.71 (t, J = 6.2 Hz, 8H, CH_2), 3.39 (br t, 8H, CH_2), 3.48 (s, J = 5.8 Hz, 8H, CH_2), 3.76 (s, 12H, OCH_3), 4.59

(t, J = 7.2 Hz, 8H, CH_2), 7.14 (t, J = 7.7 Hz, 4H, ArH), 7.35 (d, J = 5.8 Hz, 4H, ArH), 7.79 (br t, 4H, NH), 7.97 (d, J = 6.0 Hz, 4H, ArH). ^{13}C NMR (500 MHz, $CDCl_3$, 25 °C): δ 29.1, 37.9 50.6, 53.5, 55.7, 63.1, 124.3, 127.2, 129.1, 132.0, 133.9, 155.6, 164.9, 167.3, 201.4. Anal. Calcd (Found) for $C_{58}H_{64}N_{10}O_{12}S_8 \cdot 2CH_2\text{-}Cl_2$: C, 47.43 (47.45); H, 4.51 (4.52); N, 9.22 (9.54) %.

Me_4R(+)BnMeH22IAM

Me_4(H22IAM)(2-mercaptothiazolide)$_4$ (1.5 g, 1.1 mmol) was dissolved in 30 mL of $CHCl_3$, to which R(+)-α-methylbenzylamine (0.5 g, 4.1 mmol) was added slowly as a solution in 5 mL of CH_2Cl_2. The mixture was stirred under a nitrogen atmosphere for 24 h, by which time TLC analysis indicated the reaction was complete. The reaction mixture was extracted with 5% citric acid to remove any remaining free amine and then loaded directly onto silica gel for purification by flash chromatography with a 0-8% MeOH in CH_2Cl_2 gradient. Removal of solvent gave the product as a beige foam. Yield: 72%. IR (film from $CDCl_3$) ν 1652, 2938, 3283, 3379 cm^{-1}. ^{1}H NMR (500 MHz, $CDCl_3$, 25 °C): δ 1.57 (d, J = 7.0 Hz, 12H, CH3), 2.68 (br m, 12H, CH_2), 3.41 (br m, 8H, CH_2), 3.67 (s, 12H, CH_3), 5.30 (m, 4H, CH), 7.07 (br t, 4H, ArH), 7.14-7.40 (br, m, 20H, ArH), 7.64 (d, 4H, J = 5.5 Hz, ArH), 7.82 (br, s, 12 H, ArH and NH). ^{13}C NMR (125 MHz, $CDCl_3$, 25 °C): δ 21.6, 37.7, 48.7, 52.8, 53.2, 62.7, 124.1, 125.8, 126.9, 127.0, 128.2, 128.4, 132.7, 133.0, 142.8, 155.1, 164.2, 165.0.

Me_4S(-)BnMeH22IAM

This compound was prepared by the same procedure as that for Me_4R(+)BnMeH22IAM, except S(-)α-methylbenzylamine was used instead of the R(+)α-methylbenzylamine enantiomer. Separation and purification were performed as described above. The ^{1}H and ^{13}C NMR were essentially identical to those of Me_4R(+)BnMeH22IAM.

H_4R(+)BnMeH22IAM

Me_4R(+)BnMeH22IAM was dissolved in 40 mL of dry, degassed CH_2Cl_2, and BBr_3 was introduced to the solution under a nitrogen atmosphere via syringe. The resulting yellow slurry was stirred for 48 h. The slurry was slowly quenched with MeOH, after which the reaction mixture was diluted with 100 mL of water. The mixture was boiled for 5 h, and then the hot water was decanted away from an oily residue remaining in the flask. The residue was dissolved in CH_2Cl_2, dried with $MgSO_4$, and filtered. The filtrate was evaporated to dryness to give an off-white solid. Yield: 85%. Elemental analysis: Found (Calcd) C, 61.66 (61.87); H, 5.99 (6.10); N, 9.73 (9.75) % for $C_{74}H_{80}N_{10}O_{12} \cdot HBr \cdot 3H_2O$. ^{1}H NMR (400 MHz, DMSO-d_6, 25 °C): δ 1.47 (d, J = 6.8 Hz, 12H, CH_3), 3.47 (br s, 4H, CH_2), 3.74 (br s, 12H, CH_2), 5.16 (br m, 4H, CH), 6.92 (t, J = 7.6 Hz, 4H, ArH), 7.28 (br m, 20H, ArH), 7.97 (d, J = 7.2 Hz, 4H, ArH), 8.16 (d, J = 7.6 Hz, 4H, ArH), 8.91 (br t, 4H, ArH), 9.18 (d, J = 7.6 Hz, 4H, NH). ^{13}C NMR (125 MHz, DMSO-d_6,25 °C): δ 22.5, 29.9, 34.9, 49.1, 52.7, 117.4, 118.6, 119.3, 126.5, 127.3, 128.8, 133.0, 134.4, 144.3, 160.2, 167.5, 167.8. Anal. Calcd (Found) for $C_{74}H_{80}N_{10}O_{12} \cdot HBr \cdot 3H_2O$: C, 61.87 (61.66); H, 6.10 (5.99); N, 9.75 (9.73) %.

H_4S(-)BnMeH22IAM

This compound was prepared using the same deprotection procedure as that for Me_4R(+) BnMeH22IAM except starting with the S(-) isomer. The ^{1}H and ^{13}C NMR are essentially identical to that of H_4R(+)BnMeH22IAM. Anal. Calcd (Found) for $C_{74}H_{82}N_{10}O_{10} \cdot HBr \cdot 2H_2O$: C, 62.66 (62.56); H, 6.04 (5.91); N, 9.87 (9.67) %.

[LnR(+)BnMeH22IAM]Cl·$x$$H_2O$ and [LnS(-)BnMeH22IAM]-Cl·$x$$H_2O$

Luminescent complexes were isolated in their protonated forms with Ln (AR purity) = Sm (99.99+ %), Eu (99.99+%), Tb (99.999%), and Dy (99.99+%) using the following general

procedure. To the ligand H_4R(+)BnMeH22IAM·HBr·3H_2O or H_4S(-)BnMeH22IAM·HBr·2H_2O (20.0 μmol) in MeOH (ca. 7 mL) was added ca. 1.05 equiv of $LnCl_3$·6H_2O. The resulting clear solution was heated to reflux temperature, and 10 equiv of sym-collidine (ca. 30 μL) was added to deprotonate the phenolic oxygens and ensure complexation. This solution was held at reflux temperature for 4 h and then allowed to cool to room temperature. Slow addition of distilled H_2O dropwise (ca. 1-5 mL) induced precipitation of the desired complexes as white solids. These were easily collected by vacuum filtration and dried to give typical yields of ca. 80%. Elemental analysis for [LnR(+)BnMeH22IAM]-Cl·*x*H_2O. Ln = Tb, *x* = 6; Calcd (Found) C, 55.48 (55.71); H, 5.66 (5.51); N, 8.74 (8.70) %. Ln = Eu, *x* = 4; Calcd (Found) C, 57.01 (57.01); H, 5.56 (5.55); N, 8.98 (8.92) %. Ln = Dy, *x* = 6; Calcd (Found) C, 55.36 (55.43); H, 5.65 (5.43); N, 8.72 (8.69) %. Ln = Sm, *x* = 6; Calcd (Found) C, 55.78 (55.85); H, 5.69 (5.57); N, 8.79 (8.91) %. Elemental analysis for [LnS(-)BnMeH22IAM]Cl·*x*H_2O. Ln = Tb, *x* = 6; Calcd (Found) C, 56.76 (56.50); H, 5.54 (5.52); N, 8.94 (8.66) %. Ln = Eu, *x* = 4; Calcd (Found) C, 57.01 (57.33); H, 5.56 (5.69); N, 8.98 (9.00) %. These complexes are highly soluble in MeOH, EtOH, DMSO, and DMF.

Physical Methods

UV-visible absorption spectra were recorded on Perkin-Elmer Lambda 9 and Lambda 19 double beam absorption spectrometers using quartz cells of 0.10 and 1.00 cm path lengths. Circular dichroism spectra were recorded on Jasco J-810 and Jasco J-710 instruments. Emission spectra were acquired on a HORIBA Jobin Yvon IBH FluoroLog-3 spectrofluorimeter, equipped with three slit double grating excitation and emission monochromators with dispersions of 2.1 nm/mm (1200 grooves/mm). Spectra were reference corrected for both the excitation light source variation (lamp and grating) and the emission spectral response (detector and grating). Quantum yields were determined by the optically dilute method[21] using the following equation:

$$Qx/Qr = [A_r(\lambda_r)/A_x(\lambda_x)][I(\lambda_r)/I(\lambda_x)]\left[n_x^2/n_r^2\right][D_x/D_r]$$

Here *A* is the absorbance at the excitation wavelength (λ), *I* is the intensity of the excitation light at the same wavelength, *n* is the refractive index, and *D* is the integrated luminescence intensity. The subscripts "*x*" and "*r*" refer to the sample and reference, respectively. In this case, quinine sulfate in 1.0 N sulfuric acid was used as the reference (Q_r = 0.546).[22]

Luminescence lifetimes were determined on two different instruments. The first was a HORIBA Jobin Yvon IBH FluoroLog-3 spectrofluorimeter, adapted for time-correlated single photon counting (TCSPC) and multichannel scaling (MCS) measurements. A submicrosecond Xenon flash lamp (Jobin Yvon, 5000XeF) or pulsed LED (IBH, NanoLED-16) was used as the light source, coupled to a double grating excitation monochromator for spectral selection. In the former case, the input pulse energy (100 nF discharge capacitance) was ca. 50 mJ, yielding an optical pulse duration of less than 300 ns at fwhm, while, for the pulsed LED system, the peak output at 340 nm had a fwhm of 10 nm and a pulse duration of ca. 800 ps. A thermoelectrically cooled single photon detection module (HORIBA Jobin Yvon IBH, TBX-04-D) incorporating a fast risetime PMT, wide bandwidth preamplifier, and picosecond constant fraction discriminator was used as the detector. Signals were acquired using an IBH DataStation Hub photon counting module, and data analysis was performed using the commercially available DAS 6 decay analysis software package from HORIBA Jobin Yvon IBH. Goodness of fit was assessed by minimizing the reduced chi squared function, χ^2, and a visual inspection of the weighted residuals.

Alternately, a home-built instrument incorporating either a pulsed N_2 laser (Oriel, 79110) at 337.1 nm or the third harmonic of a Nd: YAG (Continuum, Powerlite, 8010) at 354.7 nm was used as the excitation source. Emission was collected perpendicular to the excitation beam, and spectral selection was achieved using either a single or double grating monochromator (Spectral Products, CM 110 or Spex, FL1005, respectively). A Hamamatsu R-928 PMT was used as the detector, and signals were acquired and digitized with a Tektronix TDS754D digital oscilloscope. Data fitting was performed by nonlinear least-squares analysis with Origin 7.

In both cases, each trace contained at least 10 000 points, and the reported lifetime values result from at least three independent measurements. Typical sample concentrations for both absorption and fluorescence measurements were ca. 10^{-4}-10^{-6} M, and 1.0 cm cells in quartz suprasil or equivalent were used for all measurements.

Circularly polarized luminescence and total luminescence spectra were recorded on an instrument according to literature procedures,[23] operating in a differential photon-counting mode. The light source for excitation was a continuous wave 450 W xenon arc lamp from a Spex FluoroLog-2 spectrofluorimeter, equipped with excitation and emission monochromators with dispersions of 4 nm/mm (SPEX, 1681B). CPL measurements were performed at 295 K in MeOH or DMF with analyte concentrations of ca. 10^{-3} M.

Results

Ligand Design and Synthesis

Octadentate ligands formed with four 2-hydroxyisophthalamide chelating groups tethered by a flexible alkylamino backbone such as H22IAM have proven to be efficient ligands for the coordination of luminescent lanthanide cations.[19] The methyl group of the amide group on the open face of the ligand has been replaced, yielding the two homochiral enantiomeric R(+) or S(-) forms of a chiral benzyl methyl substituent. This then gives an enantiomerically pure chiral form of the parent complex for CPL applications. This design strategy minimizes the distance between the stereogenic centers and the lanthanide cation and should maximize the chirality of the excited-state environment for the complex and subsequent CPL effects.

UV-Visible Absorption and Circular Dichroism

The absorption spectra of the ligands are dominated by an intense transition with an apparent maximum at ca. 316 nm which upon complexation is red-shifted by ca. 30 nm, with a new absorption band at ca. 350 nm. This change is essentially invariant for each of the lanthanide complexes (Sm(III), Eu(III), Tb(III), and Dy(III)) and is attributed to deprotonation and metal coordination by the phenols.[24] A similar effect has been observed[25] with other 2-hydroxyisophthalic acid derivatives upon complexation with beryllium, and the absorption bands of the complexes reported here are very similar to those reported previously[19] for the parent octadentate 2-hydroxyisophthalamide ligand (H22IAM)(Chart 1). Circular dichroism (CD) measurements indicate that both the free ligands and their complexes are chiral in methanol solution. In particular, the ligand does not appear to have epimerized when placed in solution or when the reaction mixture was heated in the presence of base during the synthesis of the complexes.[26] Furthermore, the two enantiomeric R(+) and S(-) forms of the complexes are mirror images in their observed CD spectra, as illustrated in Figure 1 for the Tb(III) complexes.

For both the R(+) or S(-) enantiomeric forms of the complex, the UV/visible absorption and CD spectra of the different lanthanide complexes do not differ significantly, indicating the ligand centered electronic structure of the four complexes formed with the different lanthanide cations are similar. This is expected, since the metal ion electrons of the *f*-orbitals are almost

uninvolved in chemical bonding. Thus the only major structural change between the complexes of this series is the varying size of the central metal ions. By analogy to the behavior of the parent [Ln(H22IAM)] complexes,[19] the monoprotonated neutral species is likely predominant in solution.

Significantly, the lower energy absorption band for all of the complexes is located at ca. 350 nm. This band is quite broad and gives good excitation of the complexes with wavelengths of up to ca. 390 nm. For practical applications, the low energy of this excitation wavelength has the advantage of being less harmful towards biological material, whereas most of the lanthanide complexes described in the literature to date have excitation bands located at significantly higher energy, typically between 300 and 330 nm.[27,28]

Emission Spectra and Luminescence Lifetimes

Upon UV irradiation, solutions of the free ligands (ca. 10^{-4} M) emit a strong blue luminescence (apparent λ_{max} at ca. 410 nm) that can be easily detected with the naked eye. However, upon complexation this emission is replaced by the typical luminescence color arising from the corresponding lanthanide cation (red for Eu(III), green for Tb(III), yellow/gray for Dy(III), and pink-purple for Sm(III)). These colors can also be easily visualized using a standard laboratory UV lamp ($\lambda_{ex} \approx 365$ nm, Figure 2), and no loss in signal intensity over a period of several weeks was observed, indicating good stability of the complexes.

As shown in Figure 3, inspection of the emission spectra for the R(+) complexes in solution reveals the typically sharp luminescence bands, characteristic of the different lanthanide cations. Furthermore, it can be seen that each lanthanide complex possesses at least one transition that does not significantly overlap with transitions of the other complexes. Hence, as was reported[19] for the parent octadentate H22IAM complexes, the chiral derivatives reported here also allow for the sensitization of four different lanthanide complexes, in this case each active for CPL.

Luminescence efficiency has been assessed by quantum yield determinations upon ligand excitation for each of the differing complexes, with results as summarized for the R(+) form in Table 1. These values are quite similar to those previously reported[19] for the parent lanthanide complexes formed with the 2-hydroxyisophthalamide moieties as the chelating group, in particular for Tb(III), indicating the chiral substituent has only a slight effect on the photophysical properties of the ensuing complex. However, as evident from the emission spectra (Figure 3), a significant amount of ligand emission centered at ca. 410 nm is observed for the Eu, Sm, and Dy chiral derivatives, indicating the intramolecular ligand-to-lanthanide energy transfer is incomplete, in contrast to the parent H22IAM derivatives[19] and the Tb(III) complex reported here. This observation may also account for the slightly diminished quantum yield values observed here, although these complexes can still be considered as the brightest complexes with CPL activity. These intense signals are a significant advantage for practical bioanalytical applications, as it will allow for enhanced sensitivity to be obtained by improving the signal-to-noise ratio.

In addition to steady state measurements, the luminescence lifetimes of the different lanthanide complexes were determined. The resultant monoexponential decays for the R(+) form as summarized in Table 1. As expected, the values obtained for the S(-) enantiomeric form were identical within the experimental error. We also note the luminescence lifetimes were strongly influenced by the water content of the MeOH solvent, and this effect was particularly evident in the case of Eu(III), which is known to be more sensitive to the presence of OH oscillators.[13] Nonetheless, the relatively long luminescence lifetimes are an indication that the octadentate ligand scaffold provides a significant level of protection from nonradiative deactivation of the lanthanide cations by the solvent molecules. For the R(+) enantiomeric form of the Tb(III) and

Eu(III) complexes, the luminescence lifetime measurements were also performed in MeOD, which allowed an estimate of the number of bound solvent molecules to be made using the empirical Horrock's relationship[29]

$$n = A\,(k_{H} - k_{D})$$

where k_D and k_H refer to the radiative decay rates ($1/\tau$) observed in the deuterated and non-deuterated solvent, respectively, and A is an empirical constant evaluated as 8.4 ms^{-1} and 2.1 ms^{-1} for Tb(III) and Eu(III). The resulting n parameter was evaluated to be 1.0 (±0.5) and 1.2 (±0.5), respectively, suggesting a single bound solvent molecule, which would also account for the diminished quantum yields, in particular for the Eu(III) complexes, when compared to the parent H22IAM complex. However, these values may also be an overestimate, since, as discussed elsewhere by Parker et. al.,[30] the original Horrocks relationship does not account for the effect of proximate NH and CH oscillators or OH oscillators not directly coordinated to the metal ion.

Circularly Polarized Luminescence

The CPL spectra for the magnetic dipole allowed transitions of each of the complexes, [LnR(+)BnMeH22IAM], Ln = Eu, Tb, Sm, and Dy, and [LnS(-)BnMeH22IAM], Ln = Eu, Tb, were measured following excitation at a λ_{ex} of 371-376 nm in MeOH at 295 K. For Eu(III), Tb(III), and Dy(III), the transitions of interest are the $^5D_0 \rightarrow {}^7F_1$ (ca. 594 nm), $^5D_4 \rightarrow {}^7F_5$(ca. 536 nm), and $^4F_{9/2} \rightarrow {}^6H_{11/2}$ (ca. 669 nm), respectively, while, for Sm(III), there are two strong magnetically dipole allowed transitions, namely $^4G_{5/2} \rightarrow {}^6H_{7/2}$ (ca. 565 nm) and $^4G_{5/2} \rightarrow {}^6H_{5/2}$ (ca. 597 nm). Of the several sharp emission lines shown in Figure 3, these wavelengths are particularly well suited for CPL measurements since these transitions satisfy the magnetic dipole selection rule, $\Delta J = 0, \pm 1$ (except $0 \leftrightarrow 0$), where it is predicted the CPL signal should be large.[31]

As shown in Figure 4, for Eu(III) and Tb(III), respectively, and in Figure 5, for Sm(III), CPL signals are readily apparent confirming the presence of a chiral emitting species and also display good complementarity between the R(+) and S(-) enantimoeric forms of the former complexes. All of the complexes examined exhibit relatively strong CPL activity. However, the magnitude of the luminescence dissymmetry factor, g_{lum}, which may be defined as

$$g_{lum} = \frac{\Delta I}{\frac{1}{2} I} = \frac{I_L - I_R}{\frac{1}{2}(I_L + I_R)}$$

where I_L and I_R refer to the intensity of left and right circularly polarized light, respectively, is quite different for the four metal centers, with results as summarized in Table 2.

In addition to the magnitude of the CPL signal, the line shape of the observed spectra also differs significantly for the four lanthanide complexes, as each CPL spectrum displays several peaks corresponding to crystal-field splitting of the electronic level. For Eu(III), the splitting of the ^7F_J levels is less important than those for the analogous Sm(III), Dy(III), or Tb(III) complexes, and simpler spectra are obtained which are more amenable to structural interpretation. In particular, it is of interest to note that at least four distinguishable peaks are seen in the Eu(III) $^5D_0 \rightarrow {}^7F_1$ transition (Figure 4), whereas, under tetragonal or lower symmetries, a maximum of three crystal field bands ($2J + 1$) should be observed. As a consequence, it can be concluded that there exists more than one conformation of this complex present in MeOH solution. For comparison, the CPL spectrum of the [EuR(+)BnMeH22IAM]

complex was also measured in DMF solution (Figure S1, Supporting Information) but yielded essentially identical spectra to those obtained in MeOH.

The significant CPL activity resulting from the Sm(III) and Dy(III) compounds reported here is promising for further CPL studies, and it appears this is the first reported observation of CPL activity from a Sm(III) complex formed with a chiral ligand. The addition of these two luminescent probes is an exciting prospect for multiplex measurements based on the sensitivity of these lanthanide complexes. While most of the CPL reports in the literature involving Dy (III) and Sm(III) ions refer to the measurement of racemic complexes with achiral ligands, there is one report of CPL for a chiral DOTA-based ligand Dy(III) complex with a larger CPL dissymmetry factor (g_{lum} = -0.41 at 667 nm) than reported here.[32] However, for Eu(III), the reported g_{lum} values reported herein are some of the highest ever observed, and the CPL signal from the Tb(III) complexes, while not as large, are also easily measurable. The stronger signal from the Eu(III) complex as compared to the Tb(III) compound is in accordance with previously observed behavior from other complexes with approximately C_4 symmetry.[23]

Conclusions

We report chiral, octadentate, 2-hydroxyisophthalamide ligands whose lanthanide complexes have good luminescence properties in solution and strong CPL activity. This is apparently the first system where the same ligand architecture is able to sensitize four different luminescent lanthanide cations (Sm(III), Eu(III), Tb(III), and Dy(III)), each of which with a characteristic emission band in the visible region and each of which with activity for CPL measurements (suitable for chiral multiplex conditions). This is also the first report of a Sm(III) complex formed with a chiral ligand that has CPL activity.

While the Eu(III) complex displays one of the highest CPL intensities described in the literature, its overall quantum yield is relatively modest. In contrast, the Tb(III) complex, which has a much greater quantum yield, displays a weaker CPL effect. Generally, these two effects will self-compensate, allowing the complexes to have a good compromise between luminescence intensity and CPL activity.

The complexes described here have luminescent lifetimes ranging from the microsecond to millisecond time scale. This feature facilitates the appropriate selection of a complex with a luminescence lifetime corresponding to the type of experiment or assay to be performed, which will in itself be dependent on the kinetics of the biological event taking place in solution.

Last, it is pertinent to note the existence of several coordination environments about the central metal ion for the [LnR(+)-BnMeH22IAM] complexes, as confirmed by CPL and high-resolution emission spectra for the Eu(III) complex which indicates that the emission signal corresponding to the $^5D_0 \rightarrow {}^7F_o$ electronic transition is not a unique signal. This is indicative of an environment around the lanthanide cation in which several chiral environments may be present due to some remaining flexibility of the ligand. Evidently, the coordination geometry of the ligand is not perfectly optimized for the lanthanide cation. Our efforts now focus on tighter control over the lanthanide binding to prevent different coordination modes and hence further improve the strength of the CPL signal. Similarly, the incorporation of a more water soluble chiral group is ongoing to facilitate the use of these systems in aqueous systems.

Supplementary Material

Refer to Web version on PubMed Central for supplementary material.

Acknowledgment

This research was supported by the Director, Office of Energy Research, Office of Basic Energy Sciences, Chemical Sciences Division, United States Department of Energy under Contract DE-AC03-76F00098. We acknowledge the Swiss National Science Foundation, the Leenards Foundation, and the Novartis Foundations for postdoctoral fellowships to S.P. G.M. thanks the National Institute of Health (NIH) Minority Biomedical Research Support (MBRS) Program for its support (2S06 GM008192-24AI). The authors wish to thank Ms. Francoise Muller for assistance in making CPL measurements reported in this work. This technology is licensed to Lumiphore, Inc., in which some of the authors have a financial interest.

References

(1). Lasmezas CI, Deslys J-P, Robain O, Jaegly A, Beringue V, Peyrin J-M, Fournier J-G, Hauw J-J, Rossier J, Dormont D. Science 1997;275:402. [PubMed: 8994041]

(2). Jiang P, Shen L, Yang K, Ran D, Wang J, Guo C. Dongwuxue Zazhi 2003;38:10.

(3). Coruh N, Hilmes GL, Riehl JP. J. Lumin 1988;40-41:227.

(4). Riehl JP, Richardson FS. Chem. Rev 1986;86:1.

(5). Coruh N, Riehl JP. Biochemistry 1992;31:7970. [PubMed: 1510984]

(6). Abdollahi S, Harris WR, Riehl JP. J. Phys. Chem 1996;100:1950.

(7). Mulkerrin MG. Spectrosc. Methods Determ. Protein Struct. Solution 1996:5.

(8). Kelly SM, Jess TJ, Price NC. Biochim. Biophys. Acta 2005;1751:119. [PubMed: 16027053]

(9). Bünzli J-CG. Acc. Chem. Res 2006;39:53. [PubMed: 16411740]

(10). Bünzli J-CG, Piguet C. Chem. Soc. Rev 2005;34:1048. [PubMed: 16284671]

(11). Parker D. Chem. Soc. Rev 2004;33:156. [PubMed: 15026820]

(12). Bruchez M Jr. Moronne M, Gin P, Weiss S, Alivisatos AP. Science 1998;281(5385):2013. [PubMed: 9748157]

(13). Bünzli, J-CG.; Choppin, GR., editors. Lanthanide Probes in Life, Chemical and Earth Sciences: Theory and Practice. Elsevier; Amsterdam: 1989.

(14). Mathis G. J. Biomol. Screening 1999;4:309.

(15). Sabbatini N, Guardigli M, Lehn JM. Coord. Chem. Rev 1993;123:201.

(16). Petoud S, Bünzli J-CG, Glanzman T, Piguet C, Xiang Q, Thummel RP. J. Lumin 1999;82:69.

(17). Brittain HG, Richardson FS, Martin RB. J. Am. Chem. Soc 1976;98:8255. [PubMed: 993525]

(18). Bünzli J-CG, Piguet C. Chem. Rev 2002;102:1897. [PubMed: 12059257]

(19). Petoud S, Cohen SM, Bünzli J-CG, Raymond KN. J. Am. Chem. Soc 2003;125:13324. [PubMed: 14583005]

(20). Wagnon BK, Jackels SC. Inorg. Chem 1989;28:1923.

(21). Crosby GA, Demas JN. J. Phys. Chem 1971;75:991.

(22). Meech SR, Phillips D. J. Photochem 1983;23:193.

(23). Riehl, JP.; Muller, G. Circularly Polarized Luminescence Spectroscopy from Lanthanide Systems. In: Gschneidner, KA.; Bünzli, J-CG.; Pecharsky, VK., editors. Handbook on the Physics and Chemistry of Rare Earths. Vol. 34. North-Holland Publishing Company; Amsterdam: 2005. p. 289Chapter 220

(24). Kanamori D, Furukawa A, Okamura T-A, Yamamoto H, Ueyama N. Org. Biomol. Chem 2005;3:1453. [PubMed: 15827641]

(25). Keizer TS, Sauer NN, McCleskey TM. J. Am. Chem. Soc 2004;126:9484. [PubMed: 15291520]

(26). Paul, JM.; Potter, GA.; (Chiroscience Limited, UK). Racemization of chiral amines in the presence of metal hydroxides. PCT Int. Appl. WO 9721662. 1997.

(27). Yamada T, Shinoda S, Sugimoto H, Uenishi J-I, Tsukube H. Inorg. Chem 2003;42:7932. [PubMed: 14632510]

(28). Li M, Selvin PR. J. Am. Chem. Soc 1995;117:8132.

(29). Horrocks WD Jr. Sudnick DR. Acc. Chem. Res 1981;14:384.

(30). Beeby A, Clarkson IM, Dickins RS, Faulkner S, Parker D, Royle L, de Sousa AS, Williams JAG, Woods M. J. Chem. Soc., Perkin Trans. 2 1999;3:493.

(31). Richardson FS. Inorg. Chem 1980;19:2806.

(32). Dickins RS, Howard JAK, Maupin CL, Moloney JM, Parker D, Riehl JP, Siligardi G, Williams JAG. Chem. Eur. J 1999;5:1095.

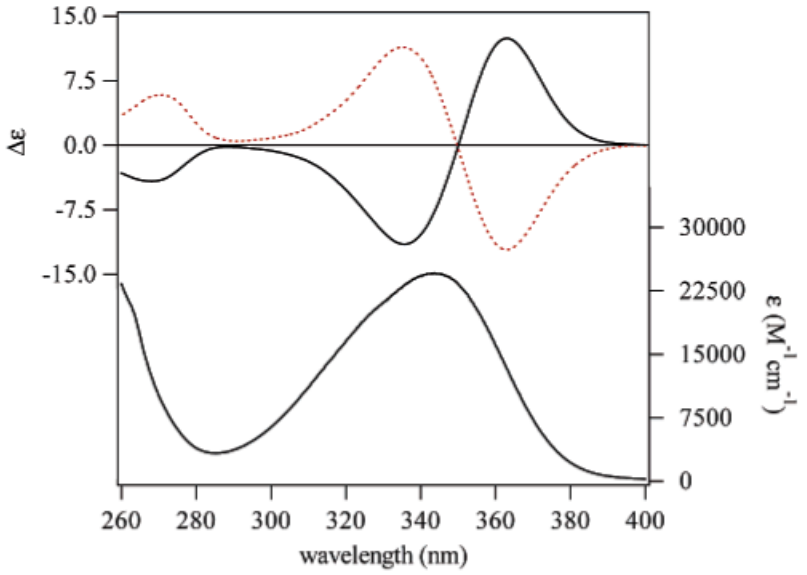

Figure 1.
UV-visible absorption (lower curve, right axis) and CD spectra (upper curves, left axis, (· · ·) = [TbR(+)BnMeH22IAM], (-) = [TbS(-)BnMeH22IAM]) for 10^{-5} M solutions of the complexes in MeOH at 298 K.

Figure 2.

Photograph of ca. 10^{-4} M solutions of the free ligand (far left) and the [LnR(+)BnMeH22IAM] complexes in MeOH with Ln = Tb, Eu, Dy, Sm from left to right, respectively, upon excitation by a standard laboratory UV lamp (λ_{exc}= 365 nm).

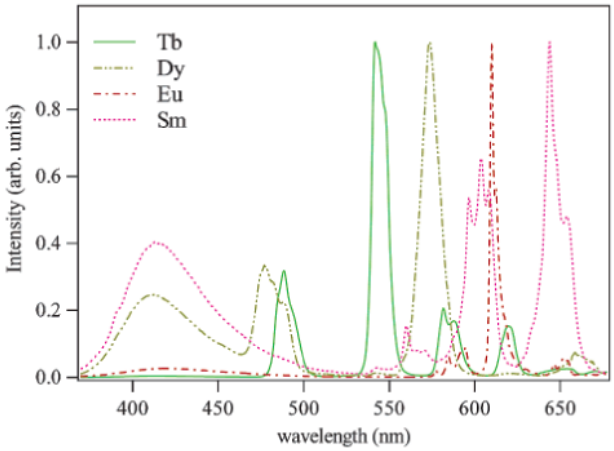

Figure 3.
Normalized emission spectra (λ_{exc} = 350 nm) for 1 × 10^{-6} M solutions of the [LnR(+) BnMeH22IAM] complexes in MeOH with Ln = Tb, Eu, Dy, Sm.

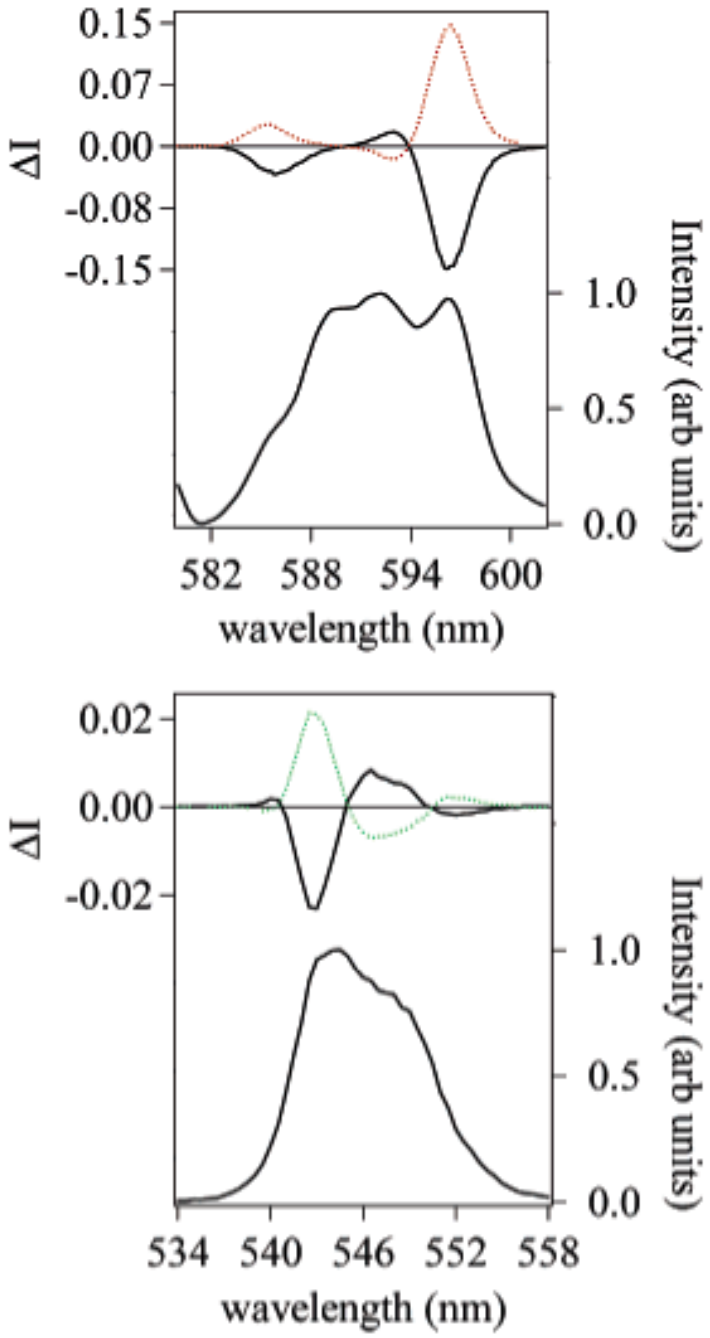

Figure 4.
Total luminescence (lower curves, right axis) and CPL spectra (upper curves, left axis, (· · ·) = [LnR(+)BnMeH22IAM], (-) = [LnS(-)BnMeH22IAM]) for 10^{-3} M solutions of the Ln = Eu (III) (top) and Ln = Tb(III) (bottom) complexes in MeOH (λ_{exc} = 371-376 nm) at 298 K.

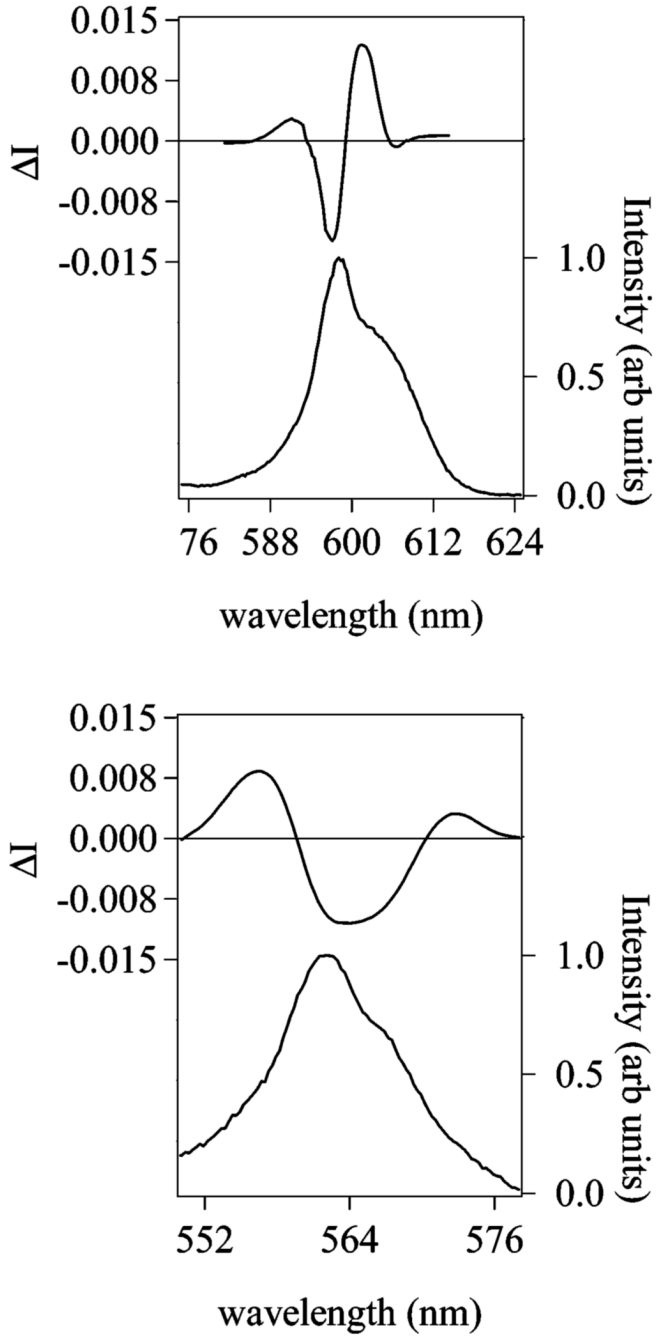

Figure 5.
Total luminescence (lower curves, right axis) and CPL spectra (upper curves, left axis) of the $^4G_{5/2} \rightarrow {}^6H_{5/2}$ and $^4G_{5/2} \rightarrow {}^6H_{7/2}$ transitions for a 10^{-3} M solution of the [Sm(R(+) BnMeH22IAM)] complex in MeOH (λ_{exc} = 371-376 nm) at 298 K.

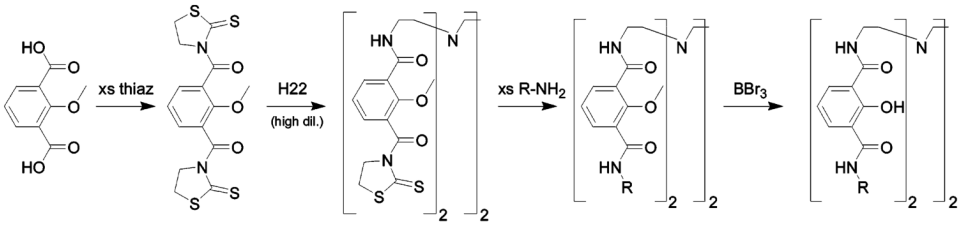

Synthesis of R(+) and S(−)BnMeH22IAM Derivatives

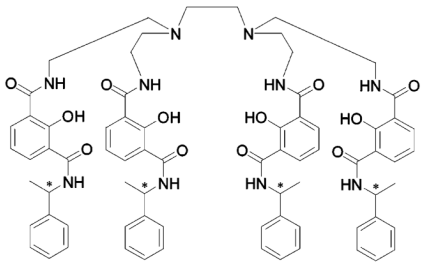

R(+)BnMeH22IAM and S(−)BnMeH22IAM

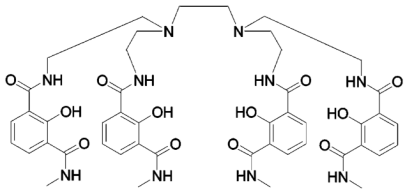

H22IAM

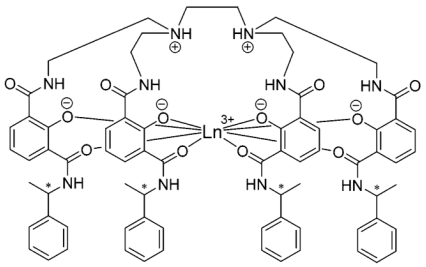

[LnR(+) and S(−)BnMeH22IAM]+

Chart 1.
Synthetic Scheme and Structure of Ligands and Complexes

Table 1

Summary of Photophysical Parameters for the [LnR(+)BnMeH22IAM] Complexes in MeOH[a]

complex	λ_{exc}, nm	quantum yield, Φ, %	luminescence lifetime, τ, μs
[TbR(+)BnMeH22IAM]	354	63.0	1271 ± 118 (1494)
[EuR(+)BnMeH22IAM]	347	2.3	784 ± 99 (1403)
[DyR(+)BnMe22IAM]	350	1.3	18 ± 3
[SmR(+)BnMeH22IAM]	350	0.8	17 ± 2

[a]Luminescence lifetimes and quantum yield values are reported here with an error of ±15%. Numbers in parentheses refer to measurements in deuterated solvent.

Table 2

Summary of CPL Results for the [Ln(BnMeH22IAM)] Complexes

complex	electronic transition	wavelength (nm)	g_{lum}
[TbR(+)BnMeH22IAM]	$^5D_4 \rightarrow {}^7F_5$	543	+0.044
[TbS(-)BnMeH22IAM]	$^5D_4 \rightarrow {}^7F_5$	543	-0.048
[EuR(+)BnMeH22IAM]	$^5D_0 \rightarrow {}^7F_1$	596	+0.298
[EuS(-)BnMeH22IAM]	$^5D_0 \rightarrow {}^7F_1$	596	-0.294
[DyR(+)BnMeH22IAM]	$^4F_{9/2} \rightarrow {}^6H_{11/2}$	669	+0.013
[SmR(+)BnMeH22IAM]	$^5G_{5/2} \rightarrow {}^6H_{7/2}$	565	-0.027
	$^4G_{5/2} \rightarrow {}^6H_{5/2}$	597	-0.028